PMAS
Proceedings of the Mongolian Academy of Sciences
Vol. 59 No 04 (232) 2019
DOI: https://doi.org/10.5564/pmas.v59i4.1292

ARTICLE

Profiles, potential and string tension of the flux tube in SU(2) and SU(3) lattice gauge theories

Sodbileg Chagdaa, Enkhtuya Galsandorj* and Battogtokh Purev

Institute of Physics and Technology, Mongolian Academy of Sciences
Ulaanbaatar, Mongolia

ARTICLE INFO: Received: 20 Aug, 2019; Accepted: 26 Feb, 2020

Abstract: *In this work, we have studied SU(2) and SU(3) gauge theories explaining the colour interaction of a quark and an antiquark, and their identical and dissimilar properties. Using both gauge theories, we have performed simulations under similar conditions and have studied the differences in the results obtained. We have compared the transverse and longitudinal profiles of the chromoelectric and chromomagnetic components of the field strength, $q\bar{q}$ potential, and temperature-dependent string tension of the flux tube. The potential between the quark and antiquark of the SU(3) theory was larger than that of the SU(2) under all temperatures. The string tension of SU(3) tends to stabilize starting from the critical temperature while that of SU(2) has a gradual decreasing feature.*

Keywords*: Lattice QCD; $q\bar{q}$ potential; gauge theory; flux tube;*

INTRODUCTION

In Quantum chromodynamics, SU(2) and SU(3) gauge theories explain the colour interaction of a quark and an antiquark. SU(2) and SU(3) gauge groups are non-abelian gauge groups. SU(2) gauge group is represented by Pauli matrix with three generations, while SU(3) gauge group is represented by Gell-Mann matrix with eight generations. SU(2) gauge theory is used to describe more simple and general case of interaction between a quark and an antiquark. However, the theory based on this group can give us a clear and important information about the interaction of a quark and an antiquark. But, the theory based on the SU(3) gauge group can express the interaction between a quark and an antiquark more precisely and completely. There are eight types of gluons that carry the interaction and eight generators of SU(3) gauge group, which correspond to them. The two theories differ with the order of the phase transition from the confined to the deconfined phase. In other words, SU(2) gauge theory has the second-order phase transition, while SU(3) gauge theory has the first order phase transition. First- and second-order phase transitions have continuous and discontinuous behaviours, respectively.

***corresponding author: enkhtuyag@mas.ac.mn** **https://orcid.org/0000-0002-2900-6890**

Vol. 59 No 04 (232) 2019
DOI: https://doi.org/10.5564/pmas.v59i4.1292

In other words, physical observables that signal the phase transition exhibit different behaviour at critical point. Physical results from these theories are similar in terms of general dependency of the physical observables on the parameters, but are different in quantity.

In order to obtain a much more exact and precise information, we had to perform simulation using the SU(3) gauge theory. Proceeding from this premise, we converted the simulation programs based on SU(2) gauge theory that we had used earlier into the program based on SU(3) gauge theory. Then, in the ref. [1], we checked our new program to assess the results generated for correctness. From this study, we observed that our new program works accurately and concluded that it can be used for more precise future studies. In the previous work [2], we analyzed and compared in detail the identical and dissimilar peculiarities of the gauge theories SU(2) and SU(3). Also, by comparing works carried out by other researchers, we analyzed the difference of physical results from these theories. In the present work, we have performed simulations with SU(3) program and sought to determine the differences in physical observables in the results from the new SU(3) program. For this reason, we made a comparison under the condition that the simulation parameters performed in this work were similar to those of the simulations performed in the previous work [3].

The rest of the paper is organized as follows. In Section 2, we provide information about the lattice definition of the observables to be measured, the details of the simulation program and the simulation parameter values. We have presented our results in Section 3, which has two subsections. The first subsection displays the comparative results of the profiles of the electric and magnetic components of the field strength in the flux tube. In the second subsection, we have computed $q\bar{q}$ potential and temperature-dependent string tension in SU(2) and SU(3) gauge theories. Finally, out conclusions are listed in Section 4 followed by references.

MATERIALS AND METHODS

Lattice measurement

Pure gauge theory with SU(3) gauge group and the standard Wilson action is used in our simulation. The measurements are performed on the lattices of size $N_{||} \times N_{\perp} \times N_{\perp} \times N_{\tau}$. We have performed simulations with the new program based on SU(3) gauge theory to see how both theories affect physical observables within flux tube. We have computed physical observables by extracting the chromoelectric and chromomagnetic components of the field strength in the flux tube from a correlation of a plaquette and the Polyakov loops as defined in the works referenced in [4, 5].

There are two Polyakov loops, located at a distance R from each other on the lattice and having oppositive directions, and they represent time propagation of the two static quarks sitting at a distance R from each other. The plaquette variable, which is at $\vec{x}$ distance from the line connecting the $q\bar{q}$ pair, with the orientation μ, ν. The six different combinations of μ and ν define the six chromoelectric and chromomagnetic components of the field strength [6]. Three space-space plaquettes correspond to the magnetic components and three space-time plaquettes correspond to the electric components. Our simulation parameters and their values are summarized in Table 1.

PMAS
Proceedings of the Mongolian Academy of Sciences
Vol. 59 No 04 (232) 2019
DOI: https://doi.org/10.5564/pmas.v59i4.1292

Table 1. Simulation parameters

Gauge groups	$N_{\|\|} \times N_{\perp}^2 \times N_\tau$	R	N_{meas}	T/T_c	β	a[fm]
SU(2)	$24 \times 12^2 \times 6$	$4a - 8a$	20000	0.75	2.35	0.14
				0.86	2.39	0.12
				0.98	2.43	0.11
				1.13	2.47	0.09
				1.29	2.51	0.08
SU(3)	$24 \times 12^2 \times 6$	$4a - 8a$	20000	0.75	5.75	0.16
				0.86	5.815	0.14
				0.98	5.79	0.12
				1.13	5.965	0.11
				1.29	6.045	0.09

From this table, we can show that for SU(2) and SU(3) gauge theories, the coupling constant's values that correspond to the same temperature are different. And when the temperatures are same, the lattice spacing of the SU(3) theory is larger than that of SU(2) theory. This means that it is a coarser lattice.

For the program based on the SU(2) gauge theory, the update algorithm was one heat bath [7-9] and four over-relaxation steps [10, 11]. For noise reduction, we used the link integration method [12] and the reference point technique [13]. And for the program based on the SU(3) gauge theory, the update algorithm was one metropolis [14] and four over-relaxation steps [10, 11]. Codes of both theories are written in C++ programming language.

RESULTS AND DISCUSSION

Longitudinal and transverse profiles

In order to study how SU(2) and SU(3) gauge theories affect the results of the physical observables, firstly, we compared the longitudinal and transverse profiles of the chromoelectric and chromomagnetic components of the field strength in the flux tube. These results are displayed in Figure 1. Longitudinal profiles at $x_\perp = 0$ of the parallel and perpendicular components of the electric and magnetic fields, $E_{||}(R,x), E_\perp(R,x), B_{||}(R,x), B_\perp(R,x)$, are displayed on the left column of Figure 1 at a given value of R separation. Their transverse profiles at $x_{||} = R/2$ are displayed on the right column of the figure at the same values of separation. Results of the SU(2) theory are denoted as red dots, while those of the SU(3) theory are in green. For comparison purpose, a lattice of size $24 \times 12^2 \times 6$,a temperature $0.98T_c$,$q\bar{q}$ separation $R = 6a$ are was chosen. The results are plotted in units of the lattice spacing. Two peaks in the figure indicate the position of a quark and an antiquark and the part we need to consider and compare is the region between the two peaks, in other words, the flux tube. From the figure, the perpendicular component of the electric field and the components of the magnetic field for the SU(2) theory are larger than that of the SU(3). For parallel component of the electric field, results of the SU(2) is approximately equal to those of SU(3). We used an error reduction method, which we called the "link integration", in our previous code based on SU(2) theory, to decrease statistical noise. But, during conversion of code, we could not include any error reduction method in the new simulation code based on the SU(3) theory since the error reduction technique did not work. Consequently, the error bars on the plots are wider.

PMAS
Proceedings of the Mongolian Academy of Sciences
Vol. 59 No 04 (232) 2019
DOI: https://doi.org/10.5564/pmas.v59i4.1292

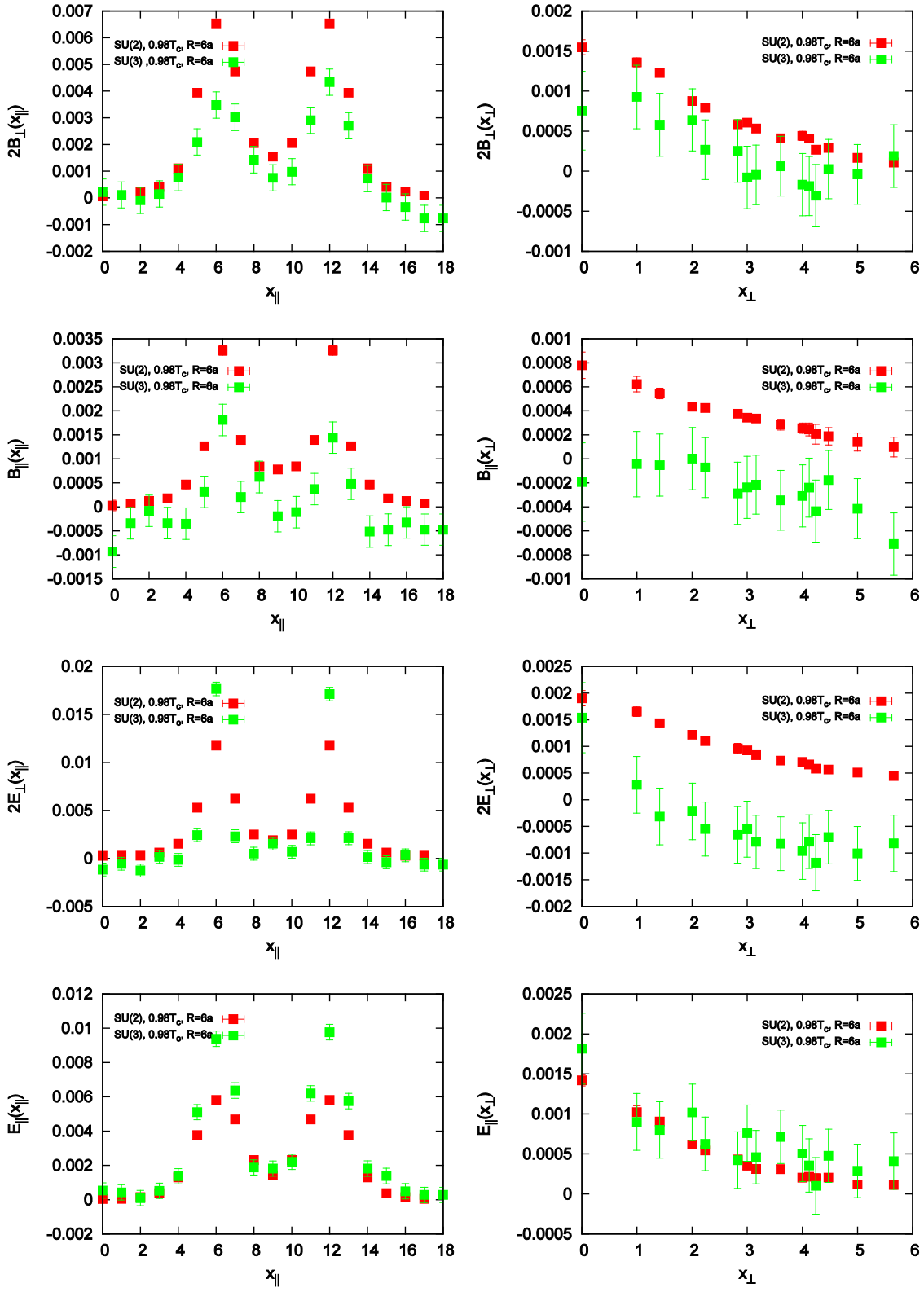

Figure 1. (Left) *Longitudinal profiles of the* $E_{||}(R,x)$, $E_{\perp}(R,x)$, $B_{||}(R,x)$, $B_{\perp}(R,x)$ *at* $(x_{||}, x_{\perp}=0)$ *and* ***(Right)*** *their transverse profiles at* $(x_{||}=R/2, x_{\perp})$ *at* $R=6a$ *from the lattice of size* $24\times12^2\times6$

$q\bar{q}$ potential and string tension

For the next physical observable, we selected the $q\bar{q}$ potential which depends on interquark distance linearly. The color-averaged potential between a quark and an

PMAS
Proceedings of the Mongolian Academy of Sciences
Vol. 59 No 04 (232) 2019
DOI: https://doi.org/10.5564/pmas.v59i4.1292

antiquark is computed from two Polyakov loop correlation

$$\langle L(\vec{0})L^{+}(\vec{R})\rangle = e^{-V(|\vec{R}|,T)/T} \qquad (1)$$

at some values of the temperature and $q\bar{q}$ separation. For the both the SU(2) and SU(3) theories, $q\bar{q}$ potential as a function of the R and T are displayed in Figure 2. Same temperatures of the SU(2) and SU(3) theory are denoted same geometrical shape ($0.75T_c$ - open rectangle, $0.86T_c$- filled rectangle, $0.98T_c$- open circle, $1.13T_c$- filled circle and $1.29T_c$- triangle). From this figure, the general trends of the $q\bar{q}$ potential which linearly increases with $q\bar{q}$ separation and decreases with the temperature were same for both SU(2) and SU(3) theories. But it is clearly observable that the potential of the SU(2) is quantitatively smaller than that of the SU(3) in this figure. This results have been plotted in units of the temperature.

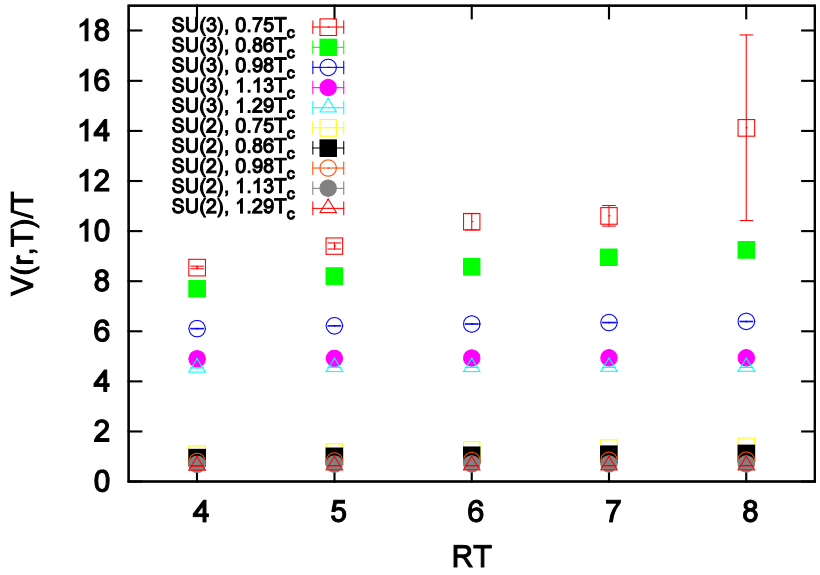

Figure 2. *$q\bar{q}$ potential as a function of $q\bar{q}$ separation at temperatures $0.75T_c - 1.29T_c$ in the SU(2) and SU(3) gauge theories. The lattice of size was $24 \times 12^2 \times 6$.*

After that, we computed the temperature-dependent string tension, $\sigma(T)$, by fitting following function on above data of the potential [15]

$$V(R,T) = V_0 - \frac{\alpha}{R} + \sigma(T)R \qquad (2)$$

with three free parameters. The potential includes a $1/R$ piece which accounts for a Coulomb type behaviour for small distances and the linear rising part. The results for the free parameters are listed in Table 2. The resulting string tension values in Table 2, normalized to their zero temperature values, are shown in Figure 3. At low temperatures, the values of string tension from SU(2) theory is slightly higher than those of SU(3). But, when the temperature increases, the difference becomes negligible. This is different from the results in ref. [16]. In this paper, the values of string tension from SU(3) theory is higher than those of SU(2) at low temperatures and this difference gets low with temperature and vanishes at the critical temperature. From this figure, we can see clearly that the string tension of SU(3) theory decreases to $0.98T_c$ and after that temperature, it stabilizes while string tension of SU(2) theory decreases to $1.13T_c$ and increases at $1.29T_c$.

PMAS
Proceedings of the Mongolian Academy of Sciences
Vol. 59 No 04 (232) 2019
DOI: https://doi.org/10.5564/pmas.v59i4.1292

Table 2. Results for the string tension in the flux tube from fit of the potential to Equation 2

Gauge groups	N_τ	T/T_c	β	aV_0	$a^2\sigma(T)$	α	χ
SU(2)	6	0.75	2.35	0.91(26)	0.069(6)	0.41(11)	0.3
		0.86	2.39	0.99(4)	0.024(4)	0.55(8)	0.4
		0.98	2.43	0.87(3)	0.004(4)	0.32(8)	0.07
		1.13	2.47	0.7294(8)	−0.01028(5)	0.160(2)	0.0003
		1.29	2.51	0.648(1)	−0.0010(1)	0.089(3)	0.004
SU(3)	6	0.75	5.75	1.61(54)	0.06(5)	1.7(1.3)	0.36
		0.86	5.815	1.39(5)	0.034(5)	0.98(15)	0.15
		0.98	5.79	1.106(3)	0.0005(2)	0.368(8)	0.01
		1.13	5.965	0.850(3)	−0.0018(27)	0.108(8)	0.17
		1.29	6.045	0.771(5)	−0.0007(4)	0.048(13)	0.82

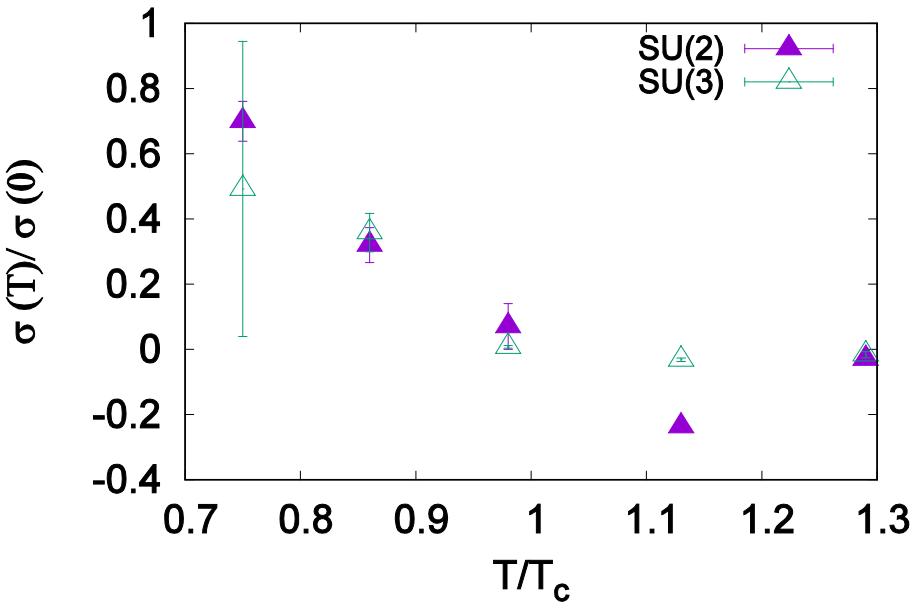

Figure 3. The string tension as obtained from fits with Equation 2, normalized to its zero temperature value

CONCLUSIONS

In this study, we have investigated the results of the two theories based on SU(2) and SU(3) gauge groups explaining the colour interaction of the quark and antiquark and compared their results. Simulation parameters were the same for both, namely, the lattice of size $24 \times 12^2 \times 6$, temperatures $0.75T_c - 1.29T_c$, number of measurement 20000, $q\bar{q}$ separation $4a - 8a$. Longitudinal and transverse profiles of the chromoelectric and chromomagnetic components of the field strength in the flux tube, the potential between a quark and an antiquark and the temperature-dependent string tension are computed and compared.

For the profiles of the flux tube, all field strength components, except the parallel electric component, for SU(3) theory were smaller than those of the SU(2) theory. On the contrary, the potential between the quark and antiquark of the SU(3) theory was larger than that of the SU(2) at all temperatures. From the results, string tension of SU(3) tends to stabilize starting from the critical temperature while that of SU(2) has a gradual decreasing feature.

Vol. 59 No 04 (232) 2019
DOI: https://doi.org/10.5564/pmas.v59i4.1292

REFERENCES

1. S. Chagdaa, B. Purev and E. Galsandorj, “Proceedings of Institute of Physics and Technology, № 44”, 3, (2017).
2. E. Galsandorj, S. Chagdaa and B. Purev, “Physics”, National University of Mongolia, 26 (490), 25, (2018).
3. S. Chagdaa, “Flux tube profiles at high temperature”, doctoral dissertation, (2008).
4. M. Fukugita and T. Niuya, Phys. Lett. 132B, 374 (1983).
5. S. Chagdaa, Pos(LATTICE 2007) 172, 4 (2007).
6. L. H. Ryder, Quantum Field Theory 2nd (Cambridge University Press, 1996).
7. M. Creutz, Phys. Rev D 21, 2308 (1980).
8. M. Creutz, Phys. Rev. Lett. 43, 553 (1979).
9. A. D. Kennedy and B. J. Pendleton, Phys. Lett. B 156, 393 (1985).
10. M. Creutz, Phys. Rev. D 36, 515 (1987).
11. P. de Forcrand and O. Jahn, (arXiv:hep-lat/0502041) (2005).
12. G. Parisi, R. Petronzio and F. Rapuano, Phys. Lett. B 128, 418 (1983).
13. R. W. Haymaker and Y. Peng, Phys. Rev. D 47, 5104 (1993).
14. N. Metropolis et al., J. Chem. Phys. 21, 1087 (1953).
15. M. Gao, Phys. Rev. D 40, 2708 (1989).
16. P. Bicudo, Phys. Rev. D82 034507, (2010).